Hindawi
Shock and Vibration
Volume 2020, Article ID 6637260, 14 pages
https://doi.org/10.1155/2020/6637260

Research Article

Traffic Capacity Assessment of the Urban Elevated Bridge after Near-Field Explosion Based on the Response Surface Method

Jinghui Jiang,[1] Chaoyi Xia ,[1] Kunpeng Wang,[2] He Xia,[1] and Qikai Sun[1]

[1]*Beijing Jiaotong University School of Civil Engineering, Beijing 100044, China*
[2]*CCCC Highway Bridges National Engineering Research Centre Co., Ltd., Beijing 100120, China*

Correspondence should be addressed to Chaoyi Xia; xiacy88@163.com

Received 3 November 2020; Revised 7 December 2020; Accepted 11 December 2020; Published 28 December 2020

Academic Editor: Giosuè Boscato

The traffic capacity of the urban elevated bridge is assessed after it is attacked by a near-field explosion, using the residual bearing capacity of the damaged pier as the assessment index. First, the finite element model of a reinforced concrete slab under near-field explosion is established by ANSYS/LS-DYNA software and compared with the experimental results, which verifies the effectiveness of the ALE (arbitrary Lagrangian–Eulerian) algorithm and the accuracy of the mesh size and material properties. Then, an "explosive-air-pier" coupling analysis model is constructed using the finite element method, and the damage of the reinforced concrete pier under three types of car bombs is evaluated. Furthermore, a response surface model for the residual bearing capacity of the pier is utilized to calculate the failure probabilities of various damage levels of the pier under the three types of car bombs and to assess the traffic capacity of the bridge after near-field explosion. The established assessment method can be used to predict the probability of bridge structural damage at various levels under different types of car bombs and to provide a reference for exploring a probability-based safety assessment method of post-explosion bridges.

1. Introduction

Duwadi and Chase [1] from the Federal Highway Administration (FHWA) pointed out that the bridge is vulnerable to physical, biological, chemical, and radiological attacks in addition to natural hazards. Among these attacks to the bridge, explosion is always a powerful but sudden action. In April 2007, in California of the United States, a tanker truck caught fire and exploded near the San Francisco-Oakland Bay Bridge, destroying the bridge structure and paralyzing the transportation hub. In February 2013, in Henan Province of China, a truck carrying fireworks and firecrackers exploded on the Yichang Bridge, causing the bridge to collapse, and some vehicles fell. The accident resulted in 13 deaths and a direct economic loss of 76.32 million yuan [2]. With the increasingly frequent occurrence of explosion accidents and high potential risk of terrorist activities today, the fast assessment of urban bridge's traffic capacity after explosion to avoid heavier casualties and greater economic losses becomes more and more important.

At the end of the 20th century, with the rapid development of computers and numerical methods, the research on the bridge structure under explosion by numerical calculation became convenient. Liu et al. [3] introduced the principles and characteristics of explosion simulation and found that the bridge after explosion presented local damage. As one of the main load-bearing parts of the bridge structure, once a pier is attacked by a near-field explosion and has a severe damage, the internal forces of the structural system will be redistributed, which may lead to the collapse of the bridge. Many researchers such as Hwang et al. [4] and Shinozuka et al. [5] directly equated the bridge structure's damage level with the pier. Therefore, the damage assessment of the pier after near-field explosion is significant to comprehensive protection and antiblast design of urban bridges.

At present, the research about explosion action on the bridge mainly focuses on the deterministic finite element (FE) model for analysis. Shiravand and Parvanehro [6] evaluated the effects of explosion on a posttensioned

concrete box bridge using ANSYS-AUTODYN. Al-Smadi [7] investigated the blast response of a bridge located at the vicinity of high explosive charge using FEA software LS-DYNA. Hájek et al. [8] assessed the response of a heterogeneous concrete-based composite bridge under blast, to observe the effect of heterogeneity on the overall response of the structure. However, in these current studies, it is difficult to reflect the contingency of blast load and the randomness of structural parameters, and either to predict the probability of various damage levels to the structure from an overall perspective.

In this paper, a method to assess the traffic capacity of an urban elevated bridge after near-field explosion based on the response surface method is proposed, which can predict the probability of various levels of damage to the bridge under different types of car bombs, to provide a reference for exploring a probability-based method on evaluating the safety of the bridge after explosions.

2. Validation of the Finite Element Model

Wang et al. [9] studied the dynamic response of a reinforced concrete (RC) slab under near-field explosion through a scale model experiment. To verify the validity of the ALE algorithm and the accuracy of the mesh size and material properties used in this paper, the FE model of an RC slab under near-field explosion is established by ANSYS/LS-DYNA software and verified by comparing with the experimental results in [9].

2.1. Description of the Numerical Model. The dimension of the RC slab is 1250 mm × 1250 mm × 50 mm, with fixed constraints on the two symmetric sides and no constraints on the others, as shown in Figure 1. The equivalent mass of the explosive is 0.94 kg, and it is placed 500 mm above the slab. The dimension of the air area is 1250 mm × 1250 mm × 1000 mm. The experimental model in [9] and the finite element model in this paper are shown in Figure 2.

The reinforcement and concrete models are established separately, and the joints between them are the complete bond in simulation. The interaction between explosive, air, and RC slab is computed by the ALE algorithm. The boundary of the air is nonreflective boundary condition.

The reinforcement is calculated using the beam element (BEAM161), and the explosives, concrete, and air are all calculated using the solid element (SOLID164). The reinforcement and concrete are simulated by the Lagrange mesh (12.5 mm), and the air and explosive are simulated by the Euler mesh (25 mm).

The air is assumed to be an ideal gas by using the ∗MAT_NULL model to describe its material properties and using the ∗EOS_LINEAR_POLYNOMIAL model to characterize the state equation. For TNT explosive, the ∗MAT_HIGH_EXPLOSION_BURN model is adopted to describe the relationship between the stress and strain, and the ∗EOS_JWJ model is adopted to characterize the relationship between the pressure and volume deformation. The kinematic plastic material model ∗MAT_PLASTIC_KINEMATIC is used to describe the constitutive relation of the reinforcement. This material has its strain failure criterion: once the strain of the reinforcement element reaches the failure strain (FS = 0.12) [10], the failure element will be automatically deleted from the calculation model. The ∗MAT_CONCRETE_DAMAGE_REL3 model is adopted in concrete simulation, which has been proved successful to reflect the damage effect, strain rate effect, strain strengthening, and softening effect of concrete, and it can effectively simulate the energy dissipation mechanism of concrete structures under explosion and impact load [11]. The failure of the concrete material is defined by the keyword ∗MAT_ADD_EROSION, which is controlled by the maximum principal strain failure criterion (MXEPS = 0.06) [12].

2.2. Analysis of Numerical Simulation. The results of FE simulation are compared with the experimental results in [9], as shown in Figure 3.

The results show that the RC slab under the explosive is seriously damaged, and the average diameter of the damaged area is about 150 mm, but none of the reinforcement is broken. Besides, there are a lot of radial cracks on the slab back. By comparison, the local damage in the numerical model of RC components is in good agreement with the experimental result, and the damage characteristics of them are similar. The calculation results also indicate that the mesh size and material properties used in the model are reasonable, and the ALE algorithm can simulate the interaction between the explosion shock wave and structure effectively. The proposed numerical model of the RC slab under explosion load can predict the structure's dynamic behavior accurately.

3. Damage Assessment of the Urban Elevated Bridge Pier under Explosion Load

3.1. Explosion Risk Sources. The main risk sources of the urban elevated bridge subjected to explosion are classified into three types of car bombs [13], according to the carrying capacities of various cars. Shown in Table 1 are their corresponding TNT equivalent mass and the heights from the explosion centers to the ground.

3.2. Damage Assessment of the Urban Elevated Bridge Pier under Explosion Load. The analysis model of the urban elevated bridge pier under explosion load is composed of air, explosive, and pier. The pier is a single-column RC structure with a rectangular cross section. The height of the pier is 4 m, its cross section size is 1.5 m × 1.5 m, and the concrete grade is C30. According to the principle of ductile seismic design, the stirrup spacing is 10 cm in the vertical direction within 1 m from the top end and 1.1 m from the bottom end, and the rest of the stirrup spacing is 20 cm. The diameter of the stirrup is 1.6 cm, and its material is HRB335. The diameter of longitudinal reinforcement is 3.2 cm, and its material is

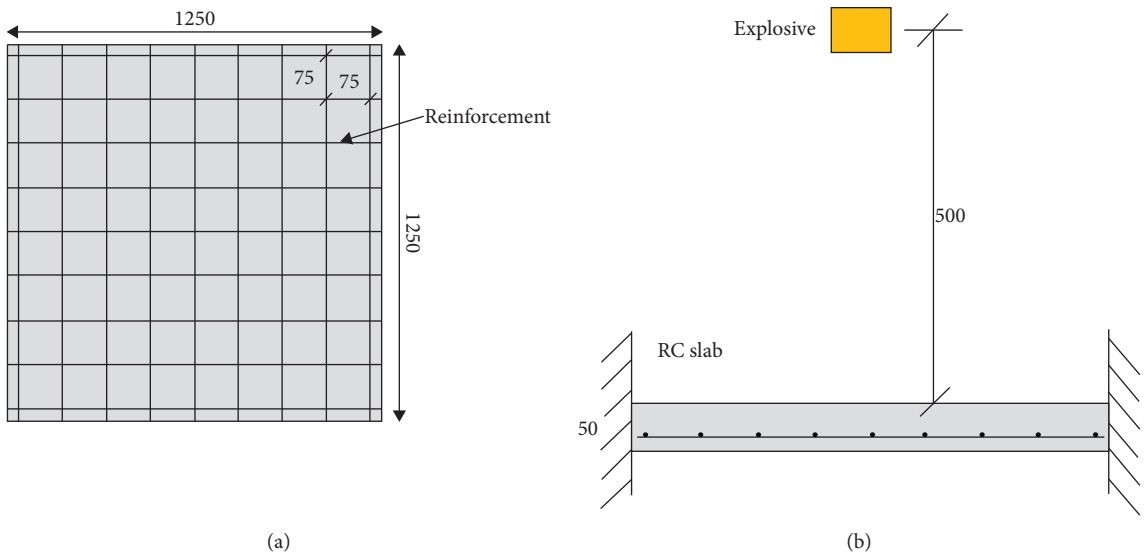

Figure 1: Dimension of the RC slab (unit: mm): (a) sectional view and (b) cross-sectional view.

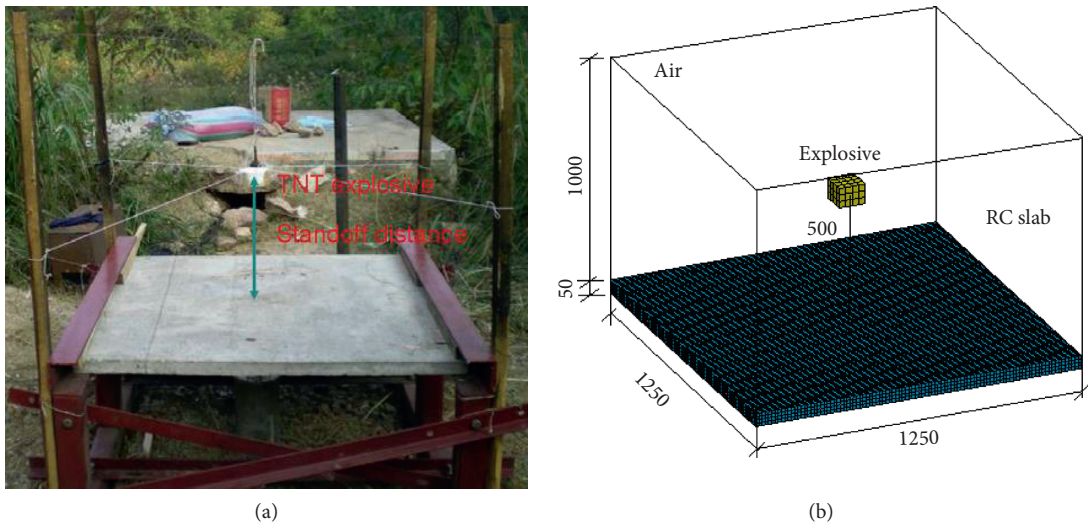

Figure 2: (a) Experimental model [9] and (b) FE model.

HRB400. The reinforcement arrangement is shown in Figure 4.

In the FE model, the explosive is placed on the central axis with a distance R from the side surface of the pier, the height from the ground is recorded as H, and the bottom of the pier is set to a fixed constraint, as shown in Figure 5. The ground boundary is set to reflective, and other boundaries of air are set to nonreflective. The mesh sizes and material properties of each part in the model are shown in Table 2, in which the mesh sizes for different elements are identical to the previously calibrated ones.

To perform damage assessment of the pier after explosion, the loading procedure on the FE model is divided into three stages, as shown in Figure 6.

First stage: the self-weight of the girders and other vertical loads are applied on the pier to simulate the initial stress state of the pier, which is realized by applying the loads at a slow rate on the top of the pier until the structure reaches a static equilibrium state.

Second stage: after stress initialization of the pier, the air and explosive parts are added in the model. The explosion load is applied on the pier by the ALE algorithm, and then the dynamic response and damage of the pier are analyzed.

According to the scale of three types of car bombs, 10 analytical cases are designed for each car-bomb type, with the explosion distances of 1.2 m, 2 m, 2.5 m, 3 m, 3.5 m, 4 m, 4.5 m, 5 m, 5.5 m, and 6 m. After attacked by three types of car bombs, the damage states of the pier under explosion distances of 1.2 m, 3.5 m, and 6 m are shown in Figure 7 and described in Table 3.

Third stage: after the post-explosion structure reaches a new state of static equilibrium, the calculation is continued

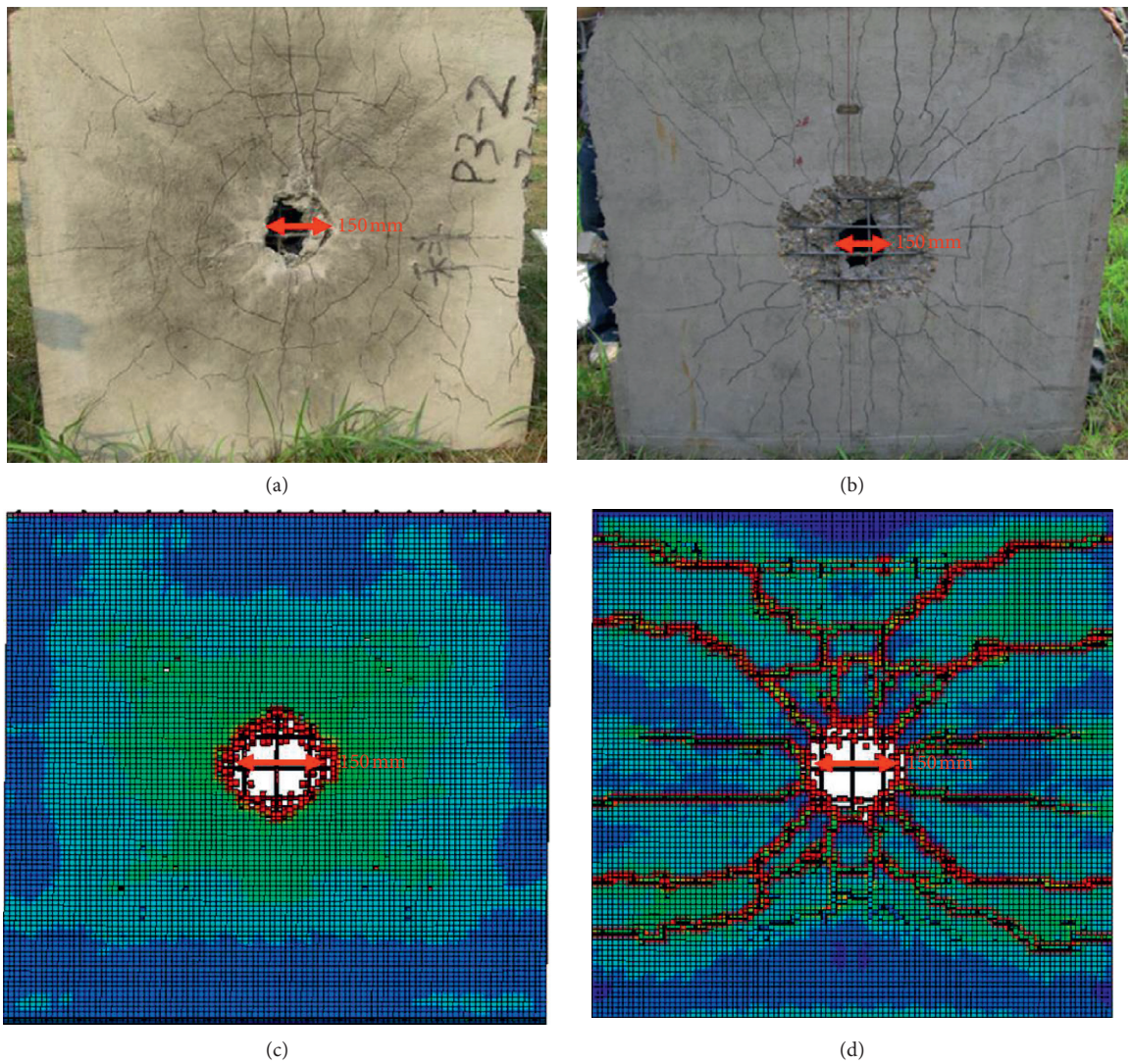

Figure 3: Comparison of experimental and numerical results: (a) front of the experimental model, (b) back of the experimental model, (c) front of the FE model, and (d) back of the FE model.

Table 1: Types and properties of car bombs.

No.	Type	TNT equivalent mass M (kg)	Height of explosion center H (m)
1#	Cargo	1000	1.0
2#	Minibus	500	0.8
3#	Normal car	200	0.5

by applying a displacement-controlled load at the pier top until the pier is destroyed, to determine the pier's residual bearing capacity [14].

To explain how to calculate the pier's residual bearing capacity, the residual axial load-time history curve of the pier is extracted at the third stage after the 3# car bomb ($M = 200$ kg, $H = 0.5$ m) attacks on the pier at 1.2 m as an analytical case, as shown in Figure 8. The value of residual bearing capacity of the pier can be determined according to the characteristics of the curve.

It is clearly found from Figure 8 that when $t = 1061.69$ ms, the axial load of the pier reaches its peak, which is defined as the residual bearing capacity of the pier ($P_{res} = 59.80$ MN). The same method is used to obtain the residual bearing capacity of the pier in the other 29 cases. Similarly, the pier without the explosion effect is calculated by applying a displacement-controlled load at the pier top, and its initial bearing capacity ($P_{ini} = 70.35$ MN) is extracted.

Based on the residual bearing capacity of the pier, the damage index D can be calculated, which is defined as [15]

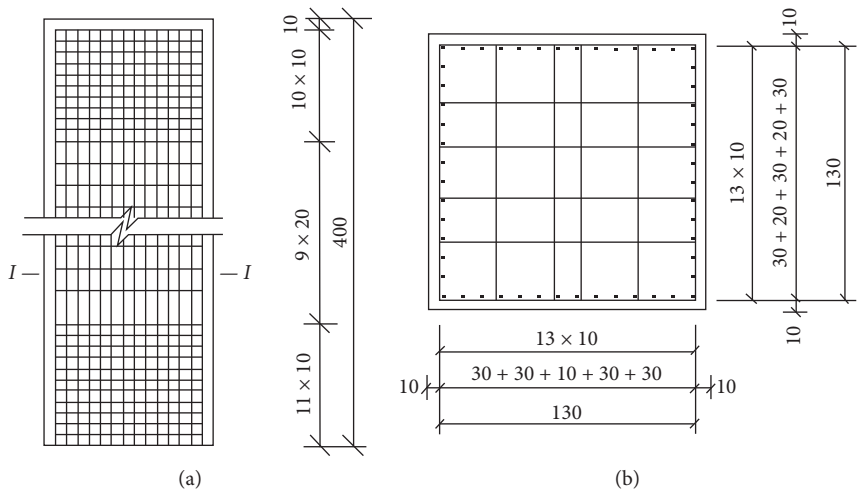

Figure 4: Dimensions of the pier (unit: cm): (a) sectional view and (b) cross-sectional view.

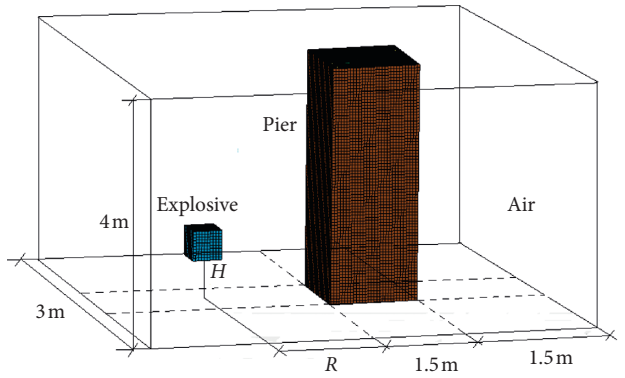

Figure 5: FE model of the pier under explosion load.

Table 2: The mesh sizes and material properties.

Part	Element	Mesh size (mm)	Material	Equation of the state	Failure criterion
Reinforcement	BEAM161	12.5	∗MAT_PLASTIC_KINEMATIC	—	FS = 0.12
Concrete	SOLID164	12.5	∗MAT_CONCRETE_DAMAGE_REL3	—	MXEPS = 0.06
Air	SOLID164_ALE	25	∗MAT_NULL	∗EOS_LINEAR_POLYNOMIAL	—
Explosive	SOLID164_ALE	25	∗MAT_HIGH_EXPLOSION_BURN	∗EOS_JWL	—

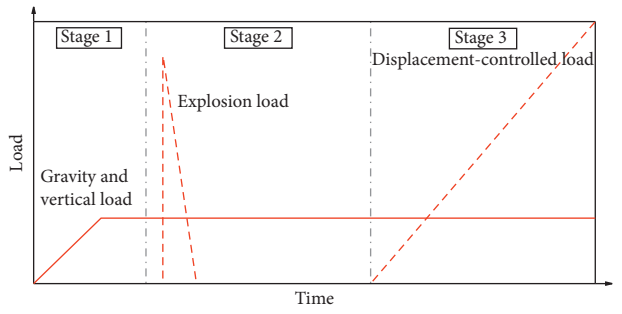

Figure 6: Three-stage loading procedure.

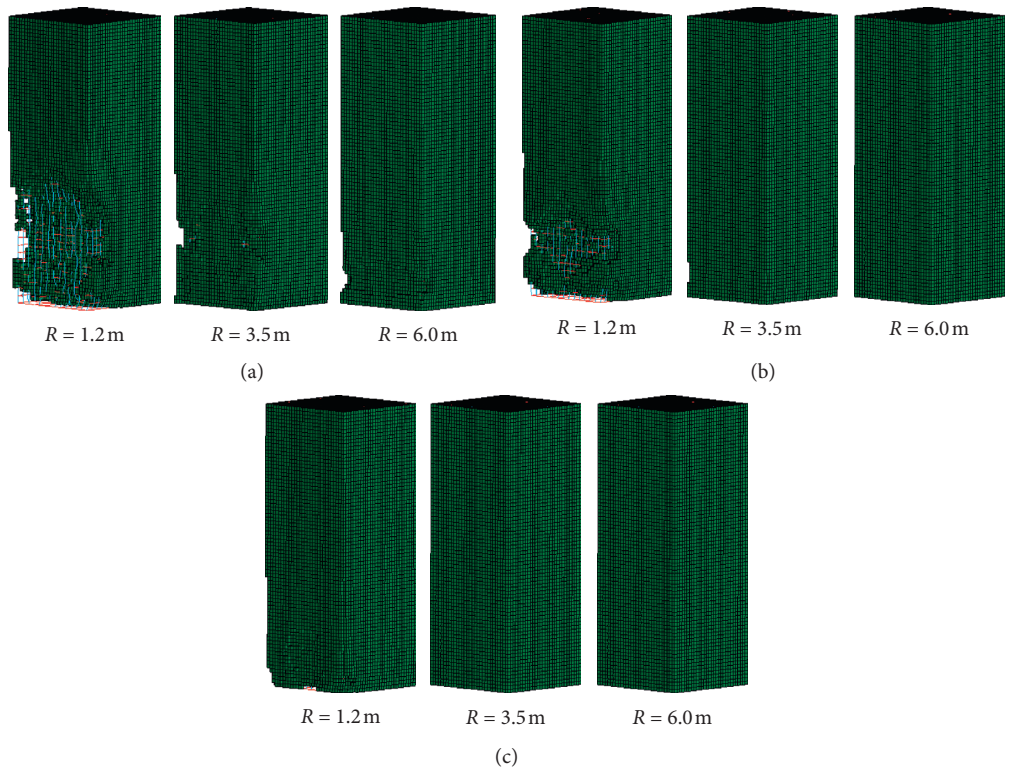

Figure 7: Several damage states of the pier under three types of car bombs: (a) 1# car bomb ($M = 1000$ kg, $H = 1.0$ m), (b) 2# car bomb ($M = 500$ kg, $H = 0.8$ m), and (c) 3# car bomb ($M = 200$ kg, $H = 0.5$ m).

Table 3: Damage states of several analytical cases.

Analytical case	R (m)	Damage states of the pier
1# car bomb	1.2	The concrete is almost completely destroyed within the height of 0 m–2 m above the ground on the near-explosion face side, and the failure rate of longitudinal reinforcement (percentage of the number of failure longitudinal reinforcements to the total number) is as high as 47.92%.
	3.5	Most of the concrete protective layer is peeled off at the height of 1 m on the near-explosion face side. A few reinforcements are exposed, but none of them reaches the failure strain.
	6.0	Part of the concrete is sheared and damaged at the pier's bottom, and no reinforcement is exposed.
2# car bomb	1.2	The concrete protective layer is almost completely peeled off at the height of 1 m on the near-explosion face side, and the failure rate of longitudinal reinforcement is 7.69%.
	3.5	The concrete in edge areas is peeled off at the height of 1 m on the near-explosion face side, and no reinforcement is exposed.
	6.0	The concrete protective layer is almost intact, and no reinforcements are exposed.
3# car bomb	1.2	Part of the concrete is sheared and damaged at the bottom of the pier, and a few of the reinforcements are exposed.
	3.5	The concrete protective layer is almost intact, and no reinforcement is exposed.
	6.0	The concrete protective layer is almost intact, and no reinforcement is exposed.

$$D = 1 - \frac{P_{\text{res}}}{P_{\text{ini}}}, \tag{1}$$

where P_{res} is the residual bearing capacity of the pier after explosion and P_{ini} is the initial bearing capacity of the pier. The corresponding damage indices D related to different explosion distances are calculated, respectively, and their relations are shown through the curves in Figure 9. The level classification of the damage indices D in the figure is quoted from [15].

As shown in Figure 9, the curve characteristics of the pier under the three types of car bombs are similar. In the initial stage of increasing the explosion distance, the damage index decreases rapidly, and then the decrease becomes slow. Under the attack of 1# car bomb, the most considerable variation of the damage index can be found than other cases, and all damage levels may appear. Under the attack of the 3# car bomb, the curve looks like a horizontal line, and the pier is only slightly damaged. It can be concluded that, under the attack of 1# car bomb, the damage index of the pier is most

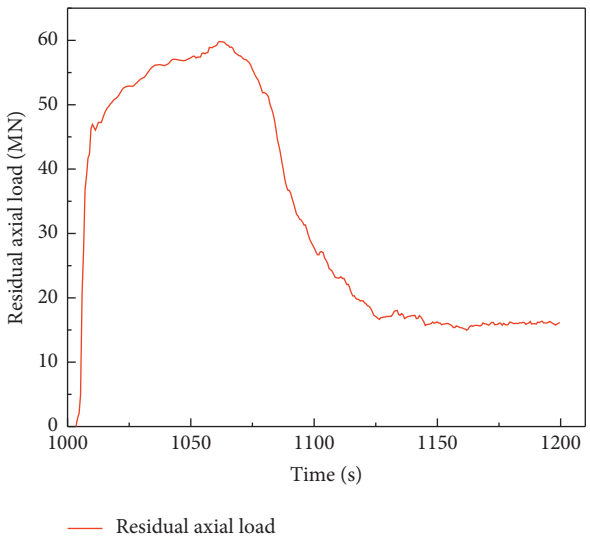

Figure 8: Residual axial load-time history curve of the pier at the third stage.

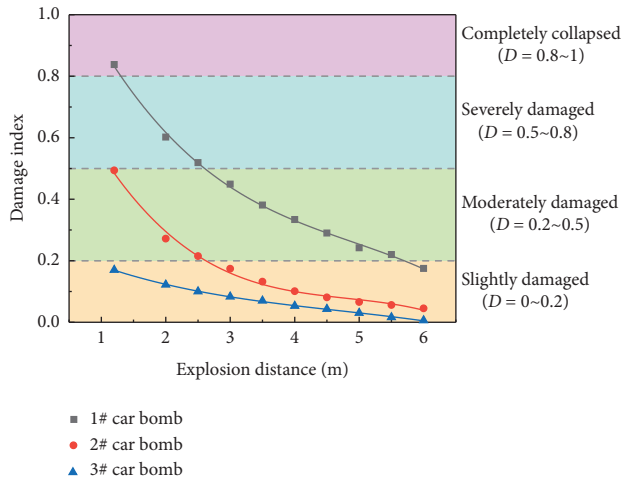

Figure 9: Damage index-explosion distance curves.

sensitive to the explosion distance, while under the 3# car bomb, the explosion distance has little effect.

Normally, the scaled distance is usually introduced to describe the intensity of explosive shock wave by combining explosive equivalent mass and explosion distance. The expression to calculate the scaled distance is

$$\overline{R} = \frac{R}{\sqrt[3]{W}}, \tag{2}$$

where R is the explosion distance and W is the explosive equivalent mass. The corresponding scaled distances are calculated under all analytical cases, and the damage index-scaled distance curve of the pier is shown in Figure 10.

From Figure 10, it is clearly seen that the dispersion of the damage index is severe when the scaled distance is less than 0.6 m/kg$^{1/3}$. Therefore, it is less suitable than direct use of explosion distance as an independent variable when rating the damage index for the pier after near-field explosion. At

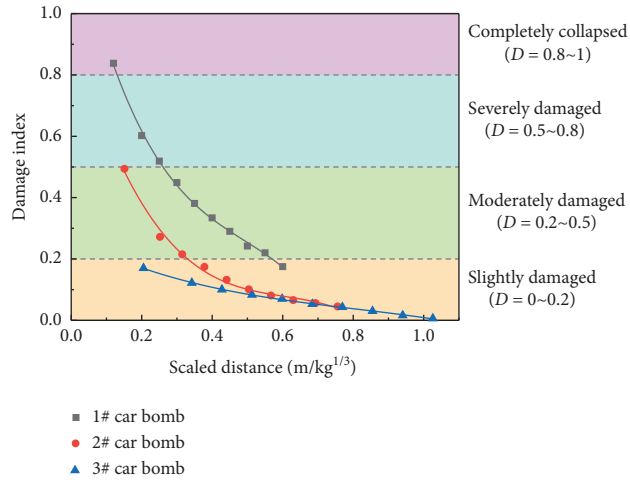

Figure 10: Damage index-scaled distance curves.

the same time, most of the similar studies [16–18] established the relationship between the explosion distance and the structural damage; the following sections of this paper will mainly study the influence of explosion distance on the damage level of the pier.

4. Traffic Capacity Assessment of the Urban Elevated Bridge after Near-Field Explosion Based on the Response Surface Method

In recent years, traffic capacity assessment of bridges after disasters has attracted the attention of some scholars. Zhou [19] summarized the calculation methods of the axial residual bearing capacity of the pier after the earthquake and assessed the bridge's traffic capacity based on the vulnerability curve of the pier. Gu [20] used the damage index to quantitatively evaluate the damage level of the pier under rockfall impact and assessed the bridge's traffic capacity by calculating the probability of the pier at various damage levels.

The response surface method is a combination of statistics and mathematics, and it performs a fitting analysis for the response problem of the objective function under the influence of multiple factors, to obtain the optimal response model. Bucher and Bourgund [21] found that the response surface model can well replace the complicated functional relationship between the structural basic parameters and responses and analyzed the reliability of the fitted response surface model. However, at present, the research on bridge's traffic capacity after explosion is still insufficient.

Referring to the assessment method of bridge's traffic capacity after the earthquake, in this section, a simple response surface mathematical model is used to replace the individual analytical case by FE model analysis.

4.1. Assessment Method of Traffic Capacity of the Urban Elevated Bridge after Near-Field Explosion. The processes to assess the traffic capacity of the urban elevated bridge after near-field explosion are shown in Figure 11. First, the main

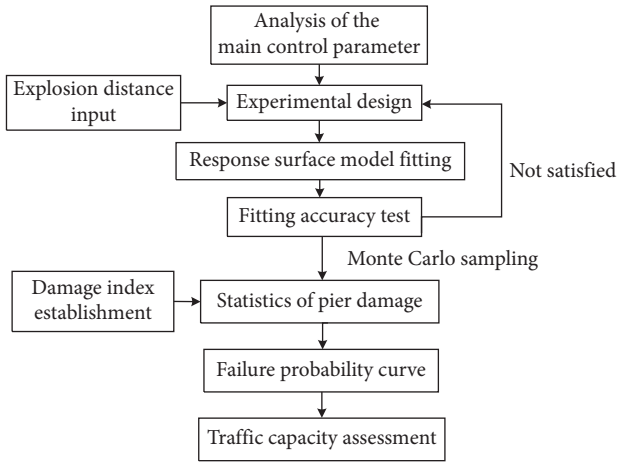

Figure 11: Traffic capacity assessment processes of the urban elevated bridge after near-field explosion.

control parameters that affect the residual bearing capacity of the pier are analyzed. Then, a series of parameter combinations are obtained through experimental design, and these parameter combinations are substituted into the FE model for calculation, based on which the response surface model is established by fitting the results. Finally, the failure probabilities at various damage levels of the pier under the attack of different car bombs are calculated by the Monte Carlo sampling method, and the vulnerability curves of the pier are plotted, through which the traffic capacity of the bridge after the near-field explosion is assessed.

To determine the traffic capacity of the bridge after explosion, the failure probability of the pier at various damage levels should be known in advance. Referring to the seismic vulnerability analysis method of the structure [22], the failure probability of the pier under explosion is defined as follows: when an explosion occurs at a distance of $R = i$ from the surface of the pier, the structure will reach a certain limit state (L_j) probability.

$$P_{ij} = P\left[S = L_j | R = i\right], \tag{3}$$

where P_{ij} is the failure probability of the structure, S is the response of the structure under explosion load, and L_j is the damage limit state. As previously mentioned, the damage level of the pier has been graded according to the damage index D so that different damage limit states (L_j) can be determined. Among them, $j = 1$, 2, 3, and 4 represents slightly damaged, moderately damaged, severely damaged, and completely collapsed of the pier, respectively.

The traffic indicator value TA is used to evaluate the traffic status of the bridge after explosion [19], which is calculated by

$$\mathrm{TA} = \sum\left(P_{ij} \times K_j\right), \tag{4}$$

where P_{ij} is the failure probability at each damage level; K_j is the weight factor corresponding to each damage level, and its value is determined by experience as 0.80 for slightly damaged, 0.65 for moderately damaged, 0.30 for severely damaged, and 0 for completely collapsed.

Considering certain allowance, the traffic of the bridge after explosion can be controlled according to different TA ranges as traffic prohibition, traffic restriction, and normal traffic operation, and the corresponding traffic rates are, respectively, specified as 0%, 50%, and 100% of the original one, as shown in Table 4.

4.2. Analysis of the Main Control Parameters. In the response surface model analysis, whether the calculation model can fit the response of the actual structure quickly and effectively depends on the selection of design parameters. If the sensitivity of the selected design parameters is low, the efficiency to predict structural damage will be reduced. Therefore, the main control parameters that affect the pier's residual bearing capacity should be analyzed quantitatively before the experimental design.

When the pier is attacked by an explosion load, its response and damage are not only influenced by the explosion distance R but also by the variations of material properties and geometric dimensions of the structure itself. The main parameters studied in this paper include concrete compressive strength f_c, longitudinal reinforcement ratio ρ_l, stirrup ratio ρ_s (proportion of stirrup volume in concrete volume), longitudinal reinforcement yield strength f_y, and stirrup yield strength f_{ys}. According to related studies [23], each main parameter is assumed to be a random variable obeying a certain distribution, as shown in Table 5.

With reference to the probability density distributions of the parameters in Table 5, the single-variable method is used to analyze the explosion of the 1# car bomb ($M = 1000$ kg, $H = 1.0$ m) at a distance of 3.5 m from the pier, to obtain its residual bearing capacity P_{res} and the initial bearing capacity P_{ini} under different analytical cases. Then, the relationship between the cases is analyzed by linear regression analysis, as shown in Table 6 and Figure 12, in which the slope k fitted for each parameter indicates the sensitivity of the residual bearing capacity of the pier to this parameter.

Table 6 also shows that the concrete compressive strength f_c, stirrup ratio ρ_s, and longitudinal reinforcement ratio ρ_l have great influence on the residual bearing capacity of the pier within the random distribution range, while the longitudinal reinforcement yield strength f_y and stirrup yield strength f_{ys} have little influence. Therefore, in the following calculation of the response surface model, only f_c, ρ_s, and ρ_l are considered as random parameters, while f_y and f_{ys} are set as fixed values ($f_y = 400$ MPa and $f_{ys} = 335$ MPa).

4.3. Experimental Design. The key step in the assessment of bridge's traffic capacity after near-field explosion is to design the experimental schemes considering the randomness of structural parameters. In this section, the central composite design (CCD) method which is the most commonly used experimental design method in the response surface method is used. This method is easy and simple in estimation of the first and second orders of the response surface numerical model, with accurate result and reasonable experiment amount [24]. The pier under the attack of each car bomb is experimented 25 times, of which the numbers of center

Table 4: Traffic control status of the bridge with respect to different TA ranges.

TA range	0–0.5	0.5–0.75	0.75–1.00
Traffic status	Traffic prohibition	Traffic restriction	Normal traffic operation
Traffic rate (%)	0	50	100

Table 5: Distribution characteristics of the main parameters.

No.	Parameter	Random variable	Distribution type	Distribution characteristics
1	Concrete compressive strength	f_c	Normal distribution	N ($\mu = 30$, COV = 0.12)
2	Longitudinal reinforcement ratio	ρ_l	Normal distribution	N ($\mu = 1.88\%$, COV = 0.055)
3	Stirrup ratio	ρ_s	Normal distribution	N ($\mu = 1.39\%$, COV = 0.055)
4	Longitudinal reinforcement yield strength	f_y	Lognormal distribution	LN ($\mu = 387$, COV = 0.07)
5	Stirrup yield strength	f_{ys}	Lognormal distribution	LN ($\mu = 387$, COV = 0.07)

Table 6: Slope k fitted in analytical cases by linear regression.

Analytical case	f_c (MPa)	ρ_l (%)	ρ_s (%)	f_y (MPa)	f_{ys} (MPa)	k
I-1	**20**					
I-2	**25**					
I-3	**30**	1.88	1.39	400	335	0.513
I-4	**35**					
I-5	**40**					
II-1		**1.42**				
II-2		**1.65**				
II-3	30	**1.88**	1.39	400	335	0.419
II-4		**2.11**				
II-5		**2.34**				
III-1			**1.06**			
III-2			**1.225**			
III-3	30	1.88	**1.39**	400	335	0.879
III-4			**1.555**			
III-5			**1.72**			
IX-1				**335**		
IX-2				**350**		
IX-3	30	1.88	1.39	**400**	335	0.26
IX-4				**450**		
IX-5				**500**		
X-1					**335**	
X-2					**350**	
X-3	30	1.88	1.39	400	**400**	0.271
X-4					**450**	
X-5					**500**	

point, axis point, and quadrant point experiments are 1 time, 8 times, and 16 times, respectively.

Referring to the random distribution characteristics of concrete compressive strength f_c, stirrup ratio ρ_s, and longitudinal reinforcement ratio ρ_l in Table 5, the probability density function curves of the parameters are drawn in Figure 13. According to the probability density distributions, in the following analysis, the range of f_c is set to 20 MPa~40 MPa, ρ_s is set to 1.06%~1.72%, and ρ_l is set to 1.42%~2.34%. Using various combinations of these random parameters, the analytical cases of the pier under the attack of three types of car bombs based on the CCD method are shown in Table 7.

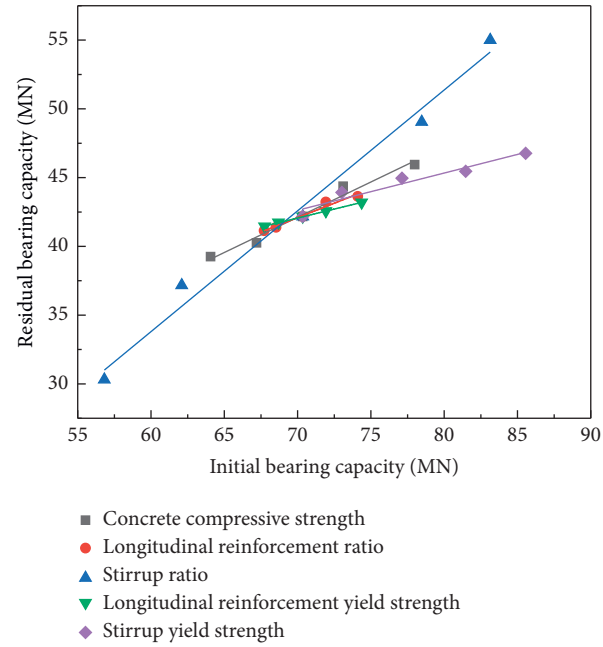

Figure 12: Linear regression graphs for different parameters.

4.4. Establishment of the Response Surface Model. The polynomial response surface model is commonly used in response surface analysis. The above-calculated results are fitted with a quadratic polynomial to form the residual bearing capacity response surface model of the pier. Its polynomial form is

$$P_{\text{res}} = a_1 + a_2 f_c + a_3 \rho_s + a_4 \rho_l + a_5 R + a_6 f_c \rho_s + a_7 f_c \rho_l + a_8 f_c R + a_9 \rho_s \rho_l + a_{10} \rho_s R + a_{11} \rho_l R + a_{12} f_c^2 + a_{13} \rho_s^2 + a_{14} \rho_l^2 + a_{15} R^2, \quad (5)$$

where f_c is the concrete compressive strength, ρ_s is the stirrup ratio, ρ_l is the longitudinal reinforcement ratio, R is the explosion distance, and a_1 to a_{15} are the partial coefficients to be determined.

According to the calculation results, a_1 to a_{15} are obtained by multivariate nonlinear fitting, as shown in Table 8.

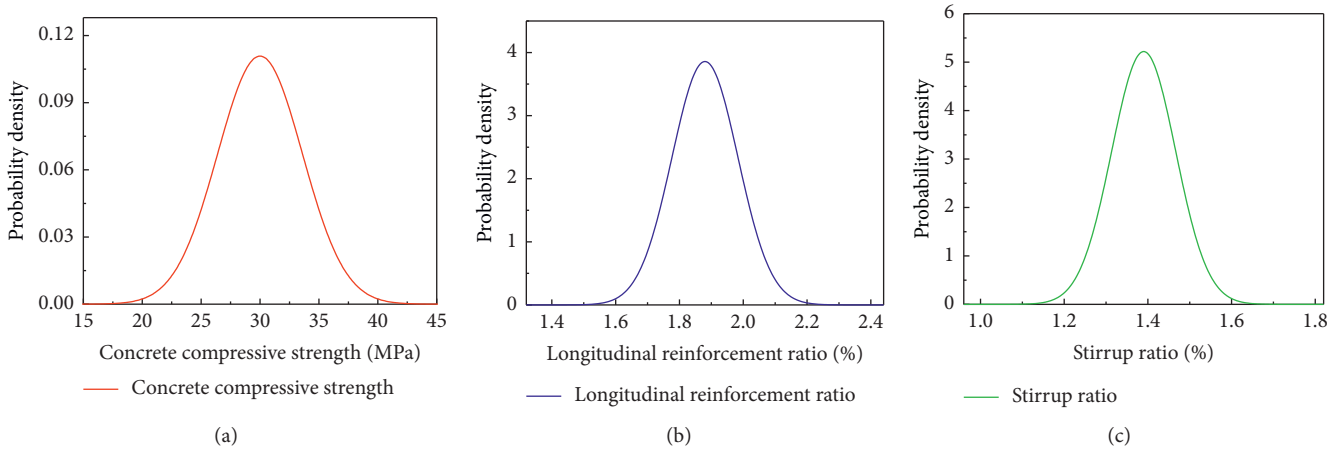

Figure 13: Probability density function: (a) concrete compressive strength, (b) longitudinal reinforcement ratio, and (c) stirrup ratio.

Table 7: Analytical cases based on the CCD method.

Analytical case	f_c (MPa)	ρ_s (%)	ρ_l (%)	R (m)	P_{res} (MN)		
					1# car bomb	2# car bomb	3# car bomb
(a)	30	1.39	1.88	3.5	42.17	61.08	64.55
(b)	40	1.39	1.88	3.5	45.94	63.82	66.17
(c)	20	1.39	1.88	3.5	39.25	56.38	61.67
(d)	30	1.72	1.88	3.5	55.00	71.67	75.91
(e)	30	1.06	1.88	3.5	30.31	50.16	52.08
(f)	30	1.39	2.34	3.5	43.63	62.95	65.76
(g)	30	1.39	1.42	3.5	41.14	58.84	62.83
(h)	30	1.39	1.88	6	58.07	67.21	69.94
(i)	30	1.39	1.88	1.2	11.43	35.58	59.80
(j)	40	1.72	2.34	6	74.50	82.88	85.86
(k)	40	1.06	2.34	6	49.95	60.09	60.22
(l)	20	1.72	2.34	6	65.65	76.18	77.10
(m)	20	1.06	2.34	6	48.16	57.84	58.06
(n)	40	1.72	1.42	6	71.17	78.91	80.91
(o)	40	1.06	1.42	6	46.19	57.42	59.98
(p)	20	1.72	1.42	6	58.27	74.18	64.45
(q)	20	1.06	1.42	6	41.45	54.02	55.13
(r)	40	1.72	2.34	1.2	14.03	47.17	78.92
(s)	40	1.06	2.34	1.2	12.13	29.66	53.05
(t)	20	1.72	2.34	1.2	12.60	41.41	68.08
(u)	20	1.06	2.34	1.2	10.65	25.05	46.97
(v)	40	1.72	1.42	1.2	13.29	44.92	69.55
(w)	40	1.06	1.42	1.2	11.71	29.32	51.32
(x)	20	1.72	1.42	1.2	12.34	41.07	66.02
(y)	20	1.06	1.42	1.2	9.11	20.40	44.90

The fitting accuracy is usually expressed by the square of the correlation coefficient. The closer the value to 1 is, the better the fitting accuracy of the response surface model is. The correlation coefficients' square values of the model under the attack of the three types of car bombs are 0.99, 0.997, and 0.977, respectively, which indicates a high fitting accuracy.

In order to compare the influence of stirrup ratio ρ_s and explosion distance R on the residual bearing capacity of the pier after the explosion, the response surface diagram under the 1# car bomb ($f_c = 30$ MPa and $\rho_l = 1.88\%$) is drawn in Figure 14. It can be found that, in the diagram, the response surface inclined toward smaller R and d_s, indicating that the closer the car bomb to the pier and the smaller the stirrup ratio d_s, the lower the residual bearing capacity of the pier and the more likely the structure will be damaged or collapsed.

According to the analysis of Figures 12 and 14, the influence level of the parameters on the residual bearing capacity of the pier is ranked as explosion distance

Table 8: Partial coefficients of the response surface model of pier's residual bearing capacity.

Partial coefficients	1# car bomb	2# car bomb	3# car bomb
a_1	−12.653	−60.207	17.056
a_2	−0.2514	0.6651	−0.2197
a_3	−1.5952	3.0529	1.8307
a_4	1.3353	−0.1389	−1.6134
a_5	−0.6212	16.168	2.1719
a_6	0.0423	0.0058	0.0628
a_7	−0.0119	−0.0025	−0.0053
a_8	0.0566	−0.0160	0.0142
a_9	−0.0056	−0.0228	0.1723
a_{10}	0.9724	0.1634	−0.1502
a_{11}	0.1187	0.0314	0.0364
a_{12}	−0.0003	−0.0059	−0.0052
a_{13}	0.0085	0.0550	−0.1109
a_{14}	−0.0147	0.0125	−0.0090
a_{15}	−1.5323	−1.7358	0.0456

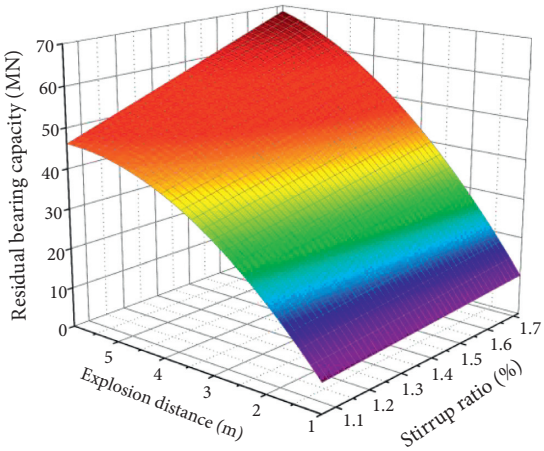

Figure 14: Response surface of pier's residual bearing capacity under 1# car bomb.

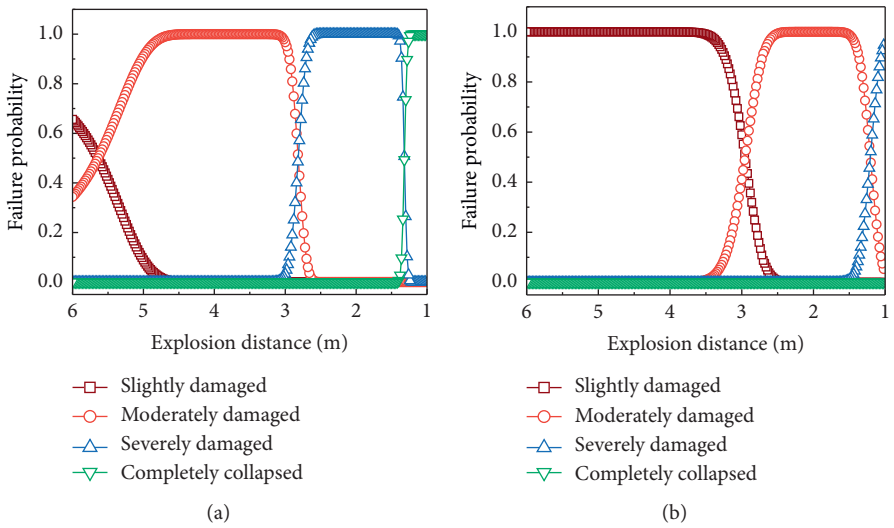

Figure 15: Continued.

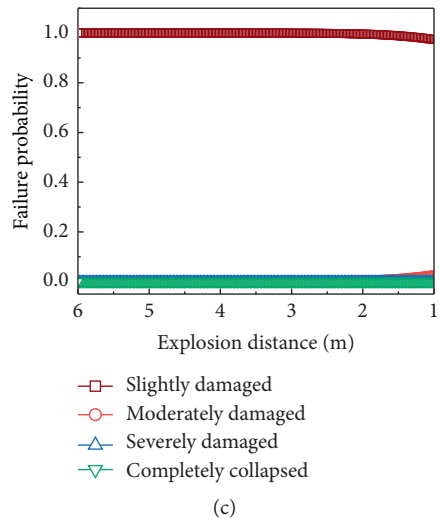

(c)

Figure 15: Failure probability curves of the pier under three types of car bombs: (a) 1# car bomb, (b) 2# car bomb, and (c) 3# car bomb.

R > stirrup ratio ρ_s > concrete compressive strength f_c > longitudinal reinforcement ratio ρ_l > stirrup yield strength f_{ys} > longitudinal reinforcement yield strength f_y.

4.5. Traffic Capacity Assessment of the Bridge after Explosion. With reference to the incremental dynamic analysis method in seismic vulnerability analysis [25], the range of the explosion distance R is set from 6 m to 1 m, and the calculation is performed at an interval of 0.02 m. The Monte Carlo method is used to sample the random variables f_c, ρ_s, and ρ_l obeying the normal distribution, and the sample size is $N = 1 \times 10^7$. Under a certain analytical case, the failure probability of the pier reaching the corresponding damage index can be expressed as

$$P_{ij} = P\left[S = L_j | R = i\right] = \frac{n_j}{N}, \tag{6}$$

where n_1, n_2, n_3, and n_4 are numbers of the samples, whose damage index D reaches slightly damaged, moderately damaged, severely damaged, and completely collapsed states at each explosion distance R.

Shown in Figure 15 are the failure probability curves of the pier under three types of car bombs.

The traffic indicator value of each analytical case can be calculated according to equation (4), and the explosion distance-traffic indicator value curves are drawn in Figure 16.

It can be seen from Figure 16 and Table 4 that, for safe traffic of the bridge after the attack of the 1# car bomb ($M = 1000$ kg, $H = 1.0$ m), when the explosion distance R is less than 2.84 m, the traffic indicator TA is less than 0.5, so no vehicle passage is allowed; when R is greater than 2.84 m and less than 6 m, TA is between 0.75 and 0.5, so vehicle passage should be restricted with a 50% traffic rate. It is noted that when the 1# car bomb explodes at a distance of 2.84 m from the pier, TA is 0.509, which is very close to the limit value 0.5 of the traffic prohibition state. Therefore, the potential hazard distance of 1# car bomb is 2.84 m.

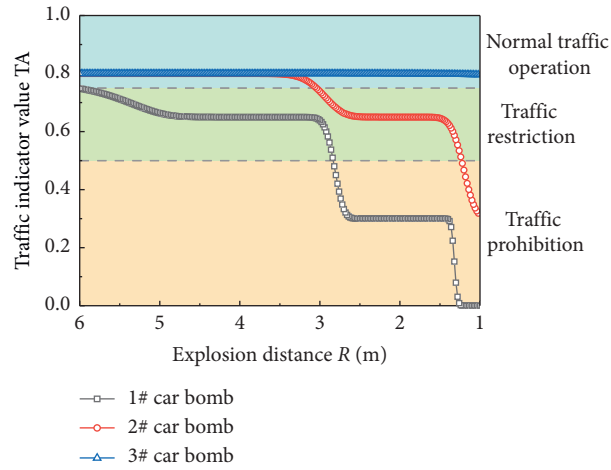

Figure 16: Explosion distance-traffic indicator value curves.

For the bridge after the attack of 2# car bomb ($M = 500$ kg, $H = 0.8$ m), when the explosion distance R is less than 1.24 m, the traffic indicator TA is less than 0.5, so the traffic on the bridge should be prohibited; when R is greater than 1.24 m and less than 3.06 m, TA is between 0.75 and 0.5, so 50% of the original traffic rate is allowed; when R is greater than 3.06 m, TA is bigger than 0.75, so there is no influence on bridge capacity, and original traffic rate is feasible. Therefore, the potential hazard distance of 2# car bomb is 1.24 m.

For the bridge after the attack of 3# car bomb ($M = 200$ kg, $H = 0.5$ m), when the explosion distance R is greater than 1 m, the traffic indicator TA remains greater than 0.75, so the bridge can be opened with the original traffic rate.

5. Conclusions

In this paper, an "explosive-air-pier" coupling model by the FE analysis method is established. By using the residual bearing capacity of the damaged pier as the assessment

index, a method for assessing the traffic capacity of the urban elevated bridge after near-field explosion based on the response surface method is proposed. The main conclusions are as follows:

(1) The damage index of the pier after near-field explosion is closely related to TNT equivalent mass and explosion distance: the greater the TNT equivalent mass of the bomb and the shorter the explosion distance are, the more seriously the pier is damaged. The pier's damage is obvious under the minibus carrying medium bomb (500 kg TNT equivalent mass) and the cargo carrying big bomb (1000 kg TNT equivalent mass). When they explode at 6.0 m away from the pier, the pier is only slightly damaged. When the explosion distance is shortened to 1.2 m, the pier is, respectively, in moderately damaged and completely collapsed states, while for the normal car carrying small bomb (200 kg TNT equivalent mass), the explosion distance has little effect on the damage index of the pier after near-field explosion.

(2) Through multiparameter analysis by the response surface model on the pier's residual bearing capacity under the three types of car bombs, the influence levels of the parameters are ranked as explosion distance R > stirrup ratio ρ_s > concrete compressive strength f_c > longitudinal reinforcement ratio ρ_l > stirrup yield strength f_{ys} > longitudinal reinforcement yield strength f_y. It shows that appropriately increasing the stirrup ratio is more conducive to improving the antiexplosion ability of the pier, and increasing the protective distance between the car bombs and the pier will significantly reduce the risk of structural collapse.

(3) For different types of car bombs, the explosion distance has a significant effect on the traffic capacity of the urban elevated bridge. For the minibus carrying 500 kg (TNT equivalent mass) bomb and the cargo carrying 1000 kg (TNT equivalent mass) bomb, the potential hazard distances that may cause severe damage or complete collapse of the structure are 1.24 m and 2.84 m, respectively. Therefore, reasonable protective measures should be taken for important piers to isolate vehicles carrying bombs beyond the potential hazard distances, in order to ensure the traffic capacity of urban elevated bridges and the safe operation of urban traffic. Once the car bomb explodes within the potential hazard distances, the traffic on the bridge should be effectively controlled.

Data Availability

The data used to support the findings of this study are included within the article.

Conflicts of Interest

The authors declare that there are no conflicts of interest regarding the publication of this paper.

Acknowledgments

This paper was supported by the Fundamental Research Funds for the Central Universities of China (2020JBM042) and Introducing Talents Base of Mitigating Wind-induced Disaster of Wind-sensitive Infrastructure (B13002).

References

[1] S. R. Duwadi and S. B. Chase, *Multiyear Plan for Bridge and Tunnel Security Research, Development, and Deployment*, FHWA-HRT-06-072, Office of Infrastructure Research and Development, Federal Highway Administration, Washington, DC, USA, 2006.

[2] Y. Gao, "The main bridge of Yichang Bridge in Henan province collapsed due to truck explosion and several vehicles fell off-CCTV network," 2015, http://news.cntv.cn/2013/02/01/ARTI1359689498633464.shtml.

[3] S. H. Liu, J. D. Wei, and Y. J. Qian, "Summary of characteristics of bridge structure explosion analysis," *Journal of Chongqing Jiaotong University*, vol. 24, no. 3, pp. 16–19, 2005.

[4] H. Hwang, J. B. Liu, and Y. H. Chiu, "Seismic fragility analysis of highway bridges," Technical Report MAEC RR-4, pp. 82–110, Mid-America Earthquake Center, The University of Memphis, Urbana, IL, USA, 2001.

[5] M. Shinozuka, M. Q. Feng, J. Lee, and T. Naganuma, "analysis of fragility curves," *Journal of Engineering Mechanics*, vol. 126, no. 12, pp. 1224–1231, 2000.

[6] M. R. Shiravand and P. Parvanehro, "Numerical study on damage mechanism of post-tensioned concrete box bridges under close-in deck explosion," *Engineering Failure Analysis*, vol. 81, pp. 103–116, 2017.

[7] Y. M. Al-Smadi, "Dynamic response of RC bridge span subjected to blast wave shock," *Procedia Manufacturing*, vol. 44, pp. 100–107, 2020.

[8] R. Hájek, K. Horníková, and M. Foglar, "Numerical assessment of the response of a heterogeneous concrete-based composite bridge deck to a near field explosion," *Engineering Structures*, vol. 225, pp. 111–206, 2020.

[9] W. Wang, D. Zhang, F. Lu et al., "Experimental study on scaling the explosion resistance of a one-way square reinforced concrete slab under a close-in blast loading," *International Journal of Impact Engineering*, vol. 49, no. 2, pp. 158–164, 2012.

[10] Y. Shi, H. Hao, and Z.-X. Li, "Numerical derivation of pressure-impulse diagrams for prediction of RC column damage to blast loads," *International Journal of Impact Engineering*, vol. 35, no. 11, pp. 1213–1227, 2008.

[11] J. M. H. Puryear, D. J. Stevens, K. A. March et al., "ALE modeling of explosive detonation on or near reinforced-concrete columns," in *Proceedings of the 12th International LS-DYNA Users Conference*, Dearborn, MI, USA, June 2012.

[12] LS-DYNA, *Keyword User's Manual*, Livermore Software Technology Corporation, Livermore, CA, USA, 2006.

[13] X. L. Kong, F. N. Jin, and M. R. Jiang, "Analysis of way and scale of terroristic raid," *Blasting*, vol. 24, no. 3, pp. 88–92, 2007.

[14] L. Liu, Z. H. Zong, and M. H. Li, "Numerical study of damage modes and assessment of circular RC pier under noncontact explosions," *Journal of Bridge Engineering*, vol. 23, no. 9, p. 04018061, 2018.

[15] J. Zhang, S. Jiang, B. Chen, C. Li, and H. Qin, "Numerical study of damage modes and damage assessment of CFST

columns under blast loading," *Shock and Vibration*, vol. 2016, Article ID 3972791, 12 pages, 2016.

[16] X. Lin, Y. X. Zhang, and P. J. Hazell, "Modelling the response of reinforced concrete panels under blast loading," *Materials & Design*, vol. 56, pp. 620–628, 2014.

[17] J. Li and H. Hao, "Numerical study of concrete spall damage to blast loads," *International Journal of Impact Engineering*, vol. 68, pp. 41–55, 2014.

[18] J. Wu, Y. Zhou, R. Zhang et al., "Numerical simulation of reinforced concrete slab subjected to blast loading and the structural damage assessment," *Engineering Failure Analysis*, vol. 118, pp. 104–926, 2020.

[19] J. J. Zhou, *Residual Capacity Assessment of Reinforced Concrete Bridge Piers Based on Fragility*, Beijing Jiaotong University, Beijing, China, 2013.

[20] X. Gu, *Study on Damage and Protective Measures of Bridge Piers under Rockfall Impact*, Southwest Jiaotong University, Chengdu, China, 2017.

[21] C. G. Bucher and U. Bourgund, "A fast and efficient response surface approach for structural reliability problems," *Structural Safety*, vol. 7, no. 1, pp. 57–66, 1990.

[22] P. Sun, F. Cui, H. Qin, and X. Hou, "Study on regular inspection frequency of bridge based on seismic vulnerability analysis," *Shock and Vibration*, vol. 2018, Article ID 7157038, 11 pages, 2018.

[23] Y. Pang, X. Wu, G. Shen et al., "Seismic fragility analysis of cable-stayed bridges considering different sources of uncertainties," *Journal of Bridge Engineering*, vol. 19, no. 4, pp. 111–122, 2014.

[24] M. A. Hariri-Ardebili, S. M. Seyed-Kolbadi, and M. Noori, "Response surface method for material uncertainty quantification of infrastructures," *Shock and Vibration*, vol. 2018, Article ID 1784203, 14 pages, 2018.

[25] M. Zain, M. Usman, S. H. Farooq, and T. Mehmood, "Seismic vulnerability assessment of school buildings in seismic zone 4 of Pakistan," *Advances in Civil Engineering*, vol. 2019, Article ID 5808256, 14 pages, 2019.